Supporting Information:

Conducting the Temperature-Dependent Conformational Change of Macrocyclic Compounds to the Lattice Dilation of Quantum Dots for Achieving Ultrasensitive Nanothermometer

Ding Zhou,[†] Min Lin,[†] Xun Liu,[†] Jing Li,[†] Zhaolai Chen,[†] Dong Yao,[†] Haizhu Sun,[‡] Hao Zhang,[†,*] and Bai Yang[†]

[†] State Key Laboratory of Supramolecular Structure and Materials, College of Chemistry, Jilin University, Changchun 130012, P. R. China, and [‡] College of Chemistry, Northeast Normal University, Changchun 130024, P. R. China.

*Address correspondence to hao_zhang@jlu.edu.cn

Figure S1. Schematic illustration of the temperature-dependent conformation change of one glucopyranose ring.

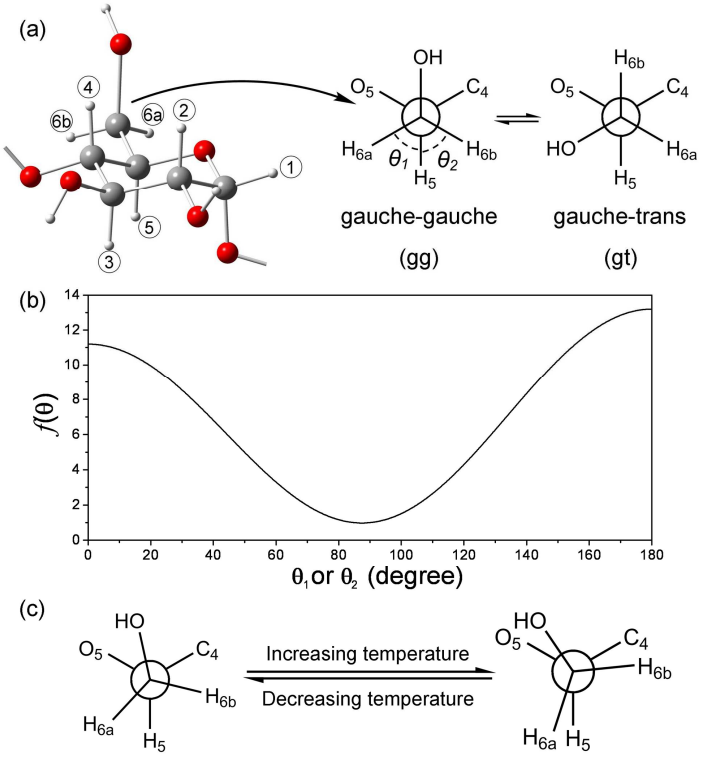

According to the previous literatures,[S1-3] there are only two staggered rotamers (gg and gt) around the C5-C6 bond (Figure S1a). Upon temperature alteration, the conformation will alter between gg and gt. The vicinal HCCH coupling constants ($J_{5,6a}$ and $J_{5,6b}$) can be used for conformational analyses with emphasis on rotamers around the C5-C6 bond in CDs. On the other hand, the J_{56a} and J_{56b} relate to the dihedral angle θ between H_5 and $H_{6a(b)}$ according to the Karplus equation:[S1,2]

$$J_{5,6a(b)} = (6.6 - 1.0\cos\theta + 5.6\cos 2\theta)(1 - \sum_{i=1}^{4} f_i \Delta x_i)$$

where θ is the dihedral angle and $(1 - \sum_{i=1}^{4} f_i \Delta x_i)$ relates to the electronegativity x of the substituents, which is temperature independent.[S2] Through NMR measurement, it is found that the vicinal coupling constants ($J_{5,6a}$ and $J_{5,6b}$) enlarge with the increase of

temperature.[S3] That is to say $f(\theta_1)$ and $f(\theta_2)$ ($f(\theta)$=6.6-1.0cosθ+5.6cos2θ) enlarge simultaneously with the increase of temperature. According to Figure S1b, θ_1 must decrease and θ_2 must increase through simple mathematic analysis. Therefore, the conformers generated by rotating the C5-C6 bond will change as shown in Figure S1c when the temperature alters, which is well consistent with the results from theoretical calculations.[S4,5]

Figure S2. (a) A series of PL spectra of α-CD-decorated CdTe QDs that are measured with the increase of temperature from -35 to 90 ºC at a step of 5 ºC (red solid), and the spectra are also measured when the temperature cools back (black dash). (b) Temperature-dependent PL peak positions of α-CD-decorated CdTe QDs.

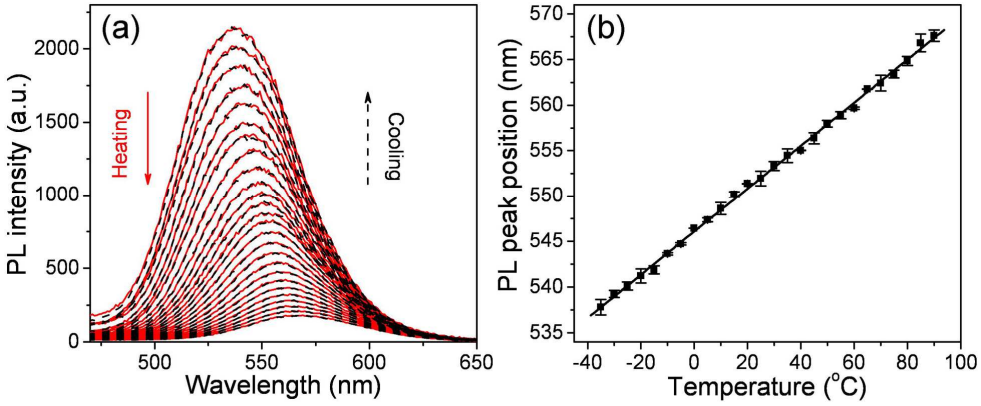

This linear relationship can be fitted as a function of $T=4.17\lambda_{max}-2275.29$ with correlation coefficient 0.9985, where λ_{max} is the PL peak position (nm), T is the temperature of the system (ºC). The characteristic sensitivity of α-CD-decorated CdTe QDs is 0.24 nm/ºC. The lower sensitivity in comparison to β-CD is understandable in terms of the structural difference in α-CD and β-CD. α-CD lacks one glucopyranose ring and therefore one sulfhydryl. It generates weaker stress toward QDs.

Figure S3. The characteristic sensitivities of β-CD- (a) and TG- (b) decorated CdTe QDs with and without N_2H_4. According to these figures, it is not found that the sensitivities of CdTe QDs relate on N_2H_4.

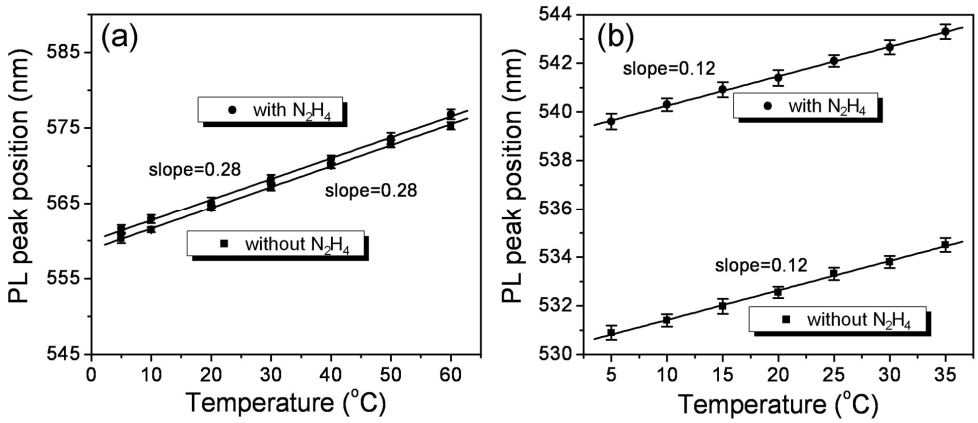

Figure S4. The theoretical calculation of the characteristic sensitivity of CdTe QDs which are decorated with conventional monothiol-ligands.

Because lots of papers have proved that the characteristic sensitivity of II-VI nanomaterials is a constant, which is relative to the size of QDs and close to those of their bulk counterpart, it just needs to confirm that the characteristic sensitivity is unchanged with the variation of the temperature for the QDs with specific size. Thus, the characteristic sensitivity will be a constant relative to the size and temperature.

The temperature-dependent energy gap of bulk semiconductor materials relates to the following Varshni relation (1):[S6]

$$E_g(T) = E_g(0) - \alpha T^2 / (T + \Theta_D) \quad \cdots\cdots (1)$$

where $E_g(T)$ is the energy gap, $E_g(0)$ is the band gap at projected at 0 K, α is a constant, and Θ_D is approximately the 0 K Debye temperature. Note that equation (1) is originally derived for the bulk crystal, yet it has been used for bulk semiconductors as well as quantum dots,[S7-9] where α and Θ_D are also constant relative to the temperature at a specific size of QDs. Moreover, there is another relationship between $E_g(T)$ and λ, which is represented in equation (2):

$$E_g(T) = h\nu = hc/\lambda \quad \cdots\cdots (2)$$

where h is Planck constant, c is light velocity, and λ is the wavelength. These two equations can be combined as equation (3):

$$\lambda = hc/(E_g(0) + \alpha\Theta_D - \alpha T - \alpha\Theta_D^2/(T + \Theta_D)) \quad \cdots\cdots (3)$$

The equation (4) could be obtained by differentiating equation (3):

$$\frac{d\lambda}{dT} = hc(\alpha - \alpha\Theta_D^2/(T+\Theta_D)^2)/(E_g(0)+\alpha\Theta_D - \alpha T - \alpha\Theta_D^2/(T+\Theta_D))^2 \quad \cdots(4)$$
$$= \lambda^2(\alpha - \alpha\Theta_D^2/(T+\Theta_D)^2)/hc$$

In which, α, h and c are constants, and λ and T are variables. In the current system, λ can be treated as a constant, because the λ only alters from 560 to 566 nm for monothiol-ligand-decorated CdTe QDs when the temperature is increased from 5 to 60 °C. Moreover, $\alpha\Theta_D^2/(T+\Theta_D)^2$, which includes the variable of T, can be also treated as a constant. To prove this consideration, the differentiation of $\alpha\Theta_D^2/(T+\Theta_D)^2$ is done, which leads to the following equation:

$$\frac{d(\alpha\Theta_D^2/(T+\Theta_D)^2)}{dT} = -2\alpha\Theta_D^2/(T+\Theta_D)^3$$

As mentioned in the previous publications,[S10] α is about 1×10^{-4} and Θ_D is about 1×10^2 K. So, when the temperature T alters from 273 to 333 K, $-2\alpha\Theta_D^2/(T+\Theta_D)^3$ should be very small. It indicates that $\alpha\Theta_D^2/(T+\Theta_D)^2$ nearly has no change, which can be looked as a constant.

Consequently, according to equation (4), $d\lambda/dT$, the characteristic sensitivity of CdTe QDs, should be constant for monothiol-ligand-decorated QDs in the investigated temperature and size range. This conclusion is well consistent with the experimental results in Figure 3c and d, according to which the relationship between λ and T is linear.

Figure S5. The comparison of surface ligand dynamics of MPA- (a) and β-CD- (b) decorated CdTe QDs by storing the newly synthesized QDs at room temperature and studying the alteration of PL intensity. The obvious PL enhancement of MPA-decorated QDs during storage reveals that the adsorption/desorption of MPA on QD surface is rather dynamic, which permits the surface atom rearrangement. In comparison, no PL enhancement is observed for β-CD-decorated QDs, showing no dynamic equilibrium of the adsorption/desorption of β-CDs on QDs.

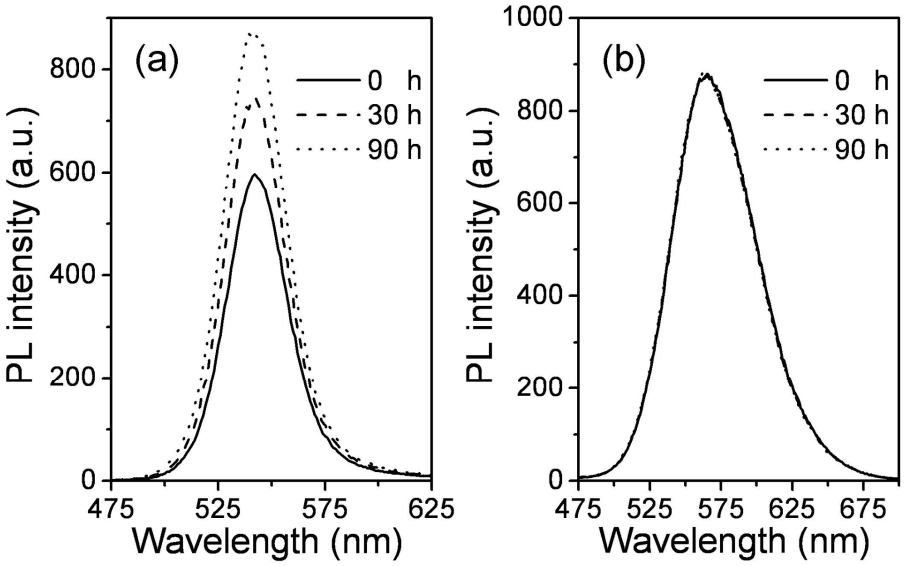

Figure S6. The calculation of the stress from the CD conformational change to CdTe QDs. The characteristic sensitivity of CdTe QDs decorated by β-CD is 0.28 nm/ºC, whereas that is 0.12 nm/ºC for the QDs decorated with MPA. So the contribution from the conformational change of β-CD is calculated to be 0.16 nm/ºC. This contribution also represents the lattice dilation of QDs by imposing a stress. In this case, the pressure coefficient of the excitonic energy gap of CdTe is about 7.9×10^{-2} eV/GPa.[S11] Therefore, the generated pressure per degree centigrade is calculated to be 8.4 MPa (*i.e.* 8.4 pN/nm^2).

Figure S7. The characteristic sensitivity of CdTe QDs decorated with the mixture of TG and β-CD. The TG to β-CD molar ratio is 1:1, which refers to the sulfhydryls. The co-decoration of CdTe QDs with β-CD and TG achieves the sensitivity of 0.17 nm/ºC, between β-CD-decorated QDs and TG-decorated ones. The decrease of β-CD ratio is reasonable to lower the contribution from the conformational change, making the sensitivity close to the inherent lattice thermal expansion coefficient of CdTe.

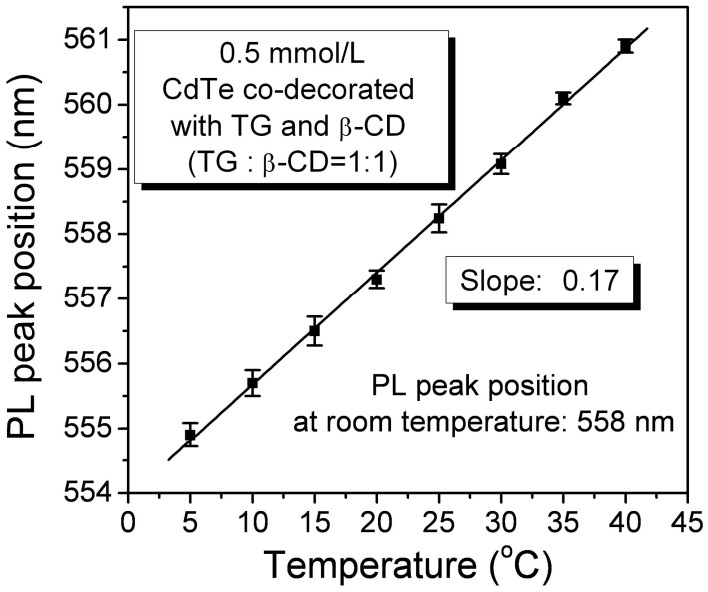

Figure S8. UV-vis absorption and PL spectra of different sized CdTe (a) and CdSe (d) QDs synthesized in high-boiling-point organic solvents (CdTe: 3.0 and 3.9 nm, CdSe: 2.6 and 4.5 nm). The shift of the peak positions of UV-vis absorption spectra of MPA- (black) and β-CD- (red) decorated CdTe (b) and CdSe (e) QDs *versus* the temperature. The shift of the peak positions of UV-vis absorption spectra of β-CD-decorated CdTe (c) and CdSe (f) QDs with different sizes *versus* the temperature.

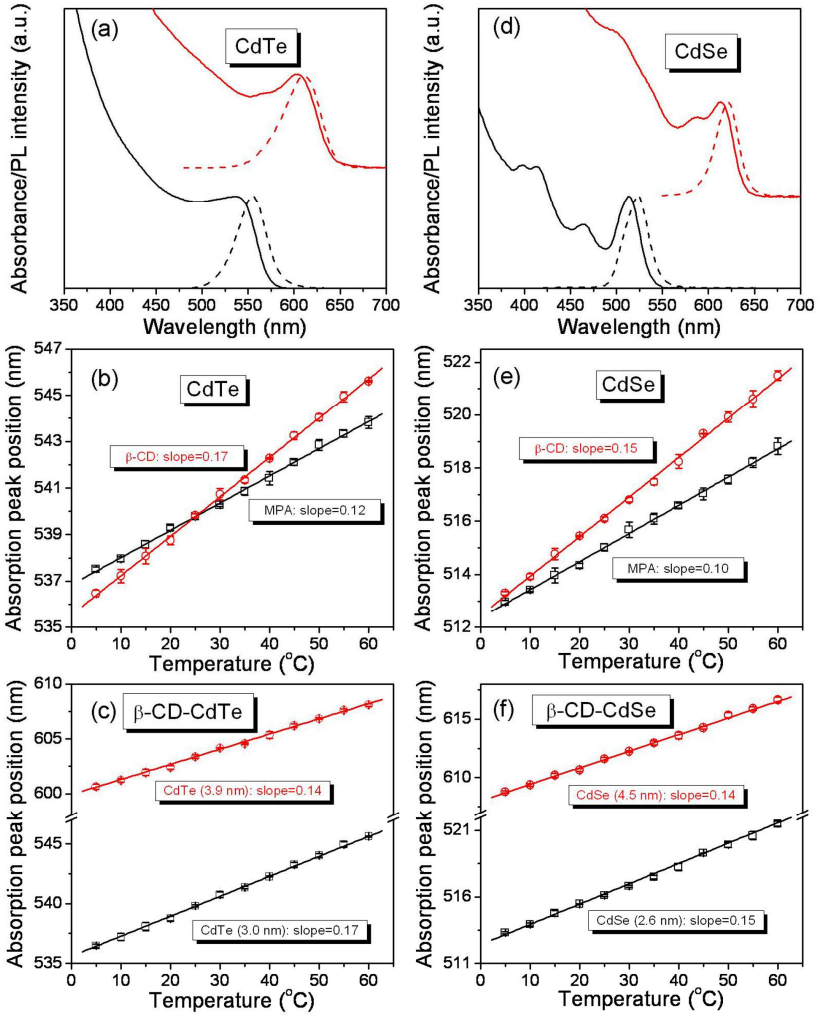

Figure S9. (a) PL spectra of α-CD-decorated CdTe QDs that are measured by storing at 90 °C for different duration. (b) UV-vis absorption spectra of α-CD-decorated CdTe QDs that are measured at 5 °C (black solid), 90 °C (red solid), 90 °C for 4 h (blue dash), and finally cooled down to 5 °C (green dash).

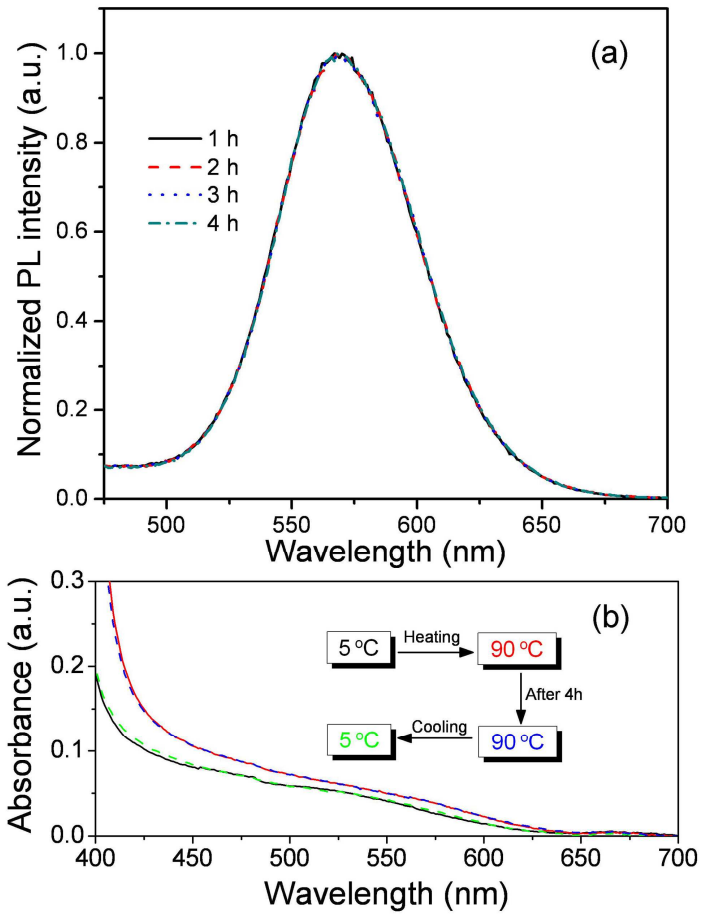

Figure S10. Comparison of the PL spectra of β-CD- (a) and MPA- (b) decorated CdTe QDs before and after storing in 10 mmol/L glutathione for 24 h.

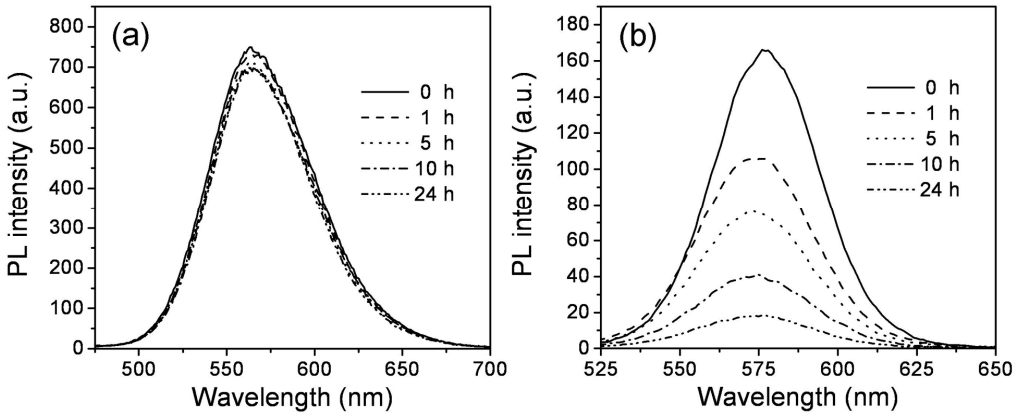

Figure S11. (a) UV-vis absorption and PL spectra of CdSe/ZnS QDs synthesized in high-boiling-point organic solvents. (b) The shift of the peak positions of PL spectra of MPA- (black) and β-CD- (red) decorated CdSe/ZnS QDs *versus* the temperature.

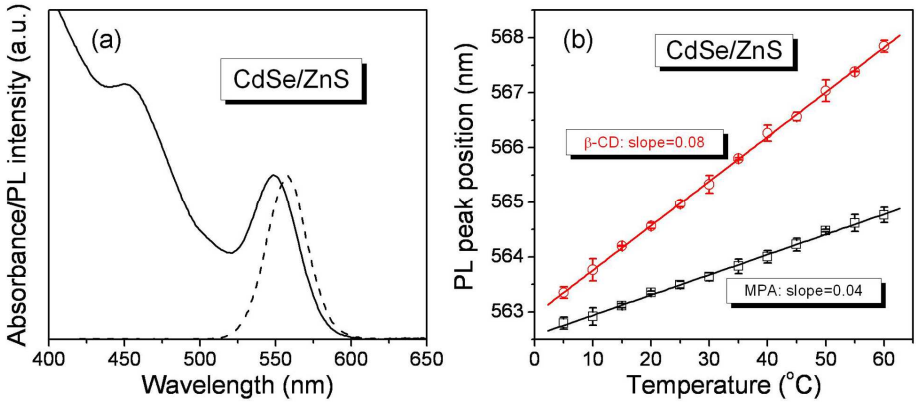

Figure S12. TEM images (a-d) and UV-vis absorption spectra (e) of the PPy-enveloped Au nanoflowers with the diameter of Au core tunable from 55 to 200 nm.

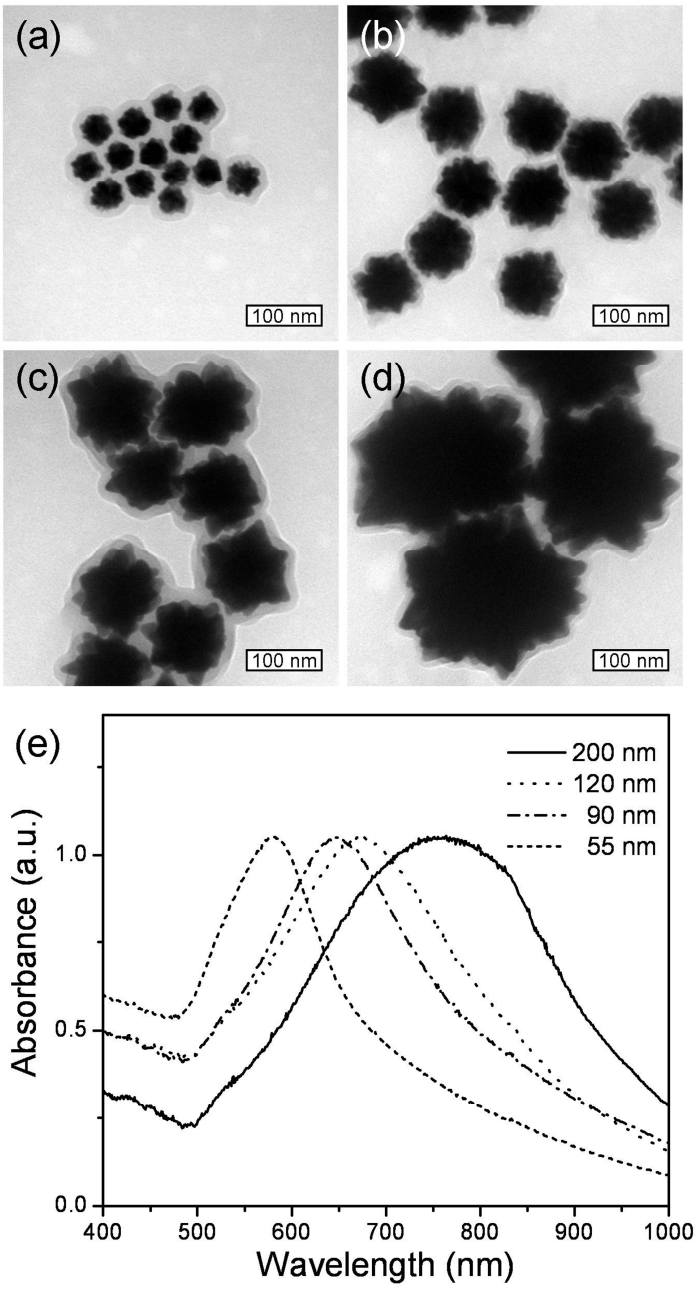

TABLE S1. The Extinction Coefficient of the Bare Au and PPy-Enveloped Au Nanoflowers *versus* the Size.

sample[a]	the extinction coefficient of the Au nanoflowers with different diameters ($M^{-1}cm^{-1}$)			
	55 nm	90 nm	120 nm	200 nm[b]
bare Au nanoflowers	9.2×10^{8}	1.2×10^{10}	3.4×10^{10}	4.6×10^{11}
PPy-enveloped Au nanoflowers	1.0×10^{9}	1.3×10^{10}	5.3×10^{10}	4.9×10^{11}

[a] The extinction coefficient of the Au nanoflowers is determined by using the method reported previously, which bases on the measurement of Au nanoflower extinction at the wavelength corresponding to their surface plasmon resonance.[S12] By comparing with the bare Au nanoflowers, the extinction coefficient of PPy-enveloped Au nanoflowers is mainly contributed to the Au core. [b] In our experiment, 200 nm PPy-enveloped Au nanoflowers are employed.

Figure S13. The PL spectra and PL images of β-CD-decorated CdTe QDs before (black solid) and after (red dash) 808 nm NIR laser irradiation. The laser power density is 3 W/cm^2.

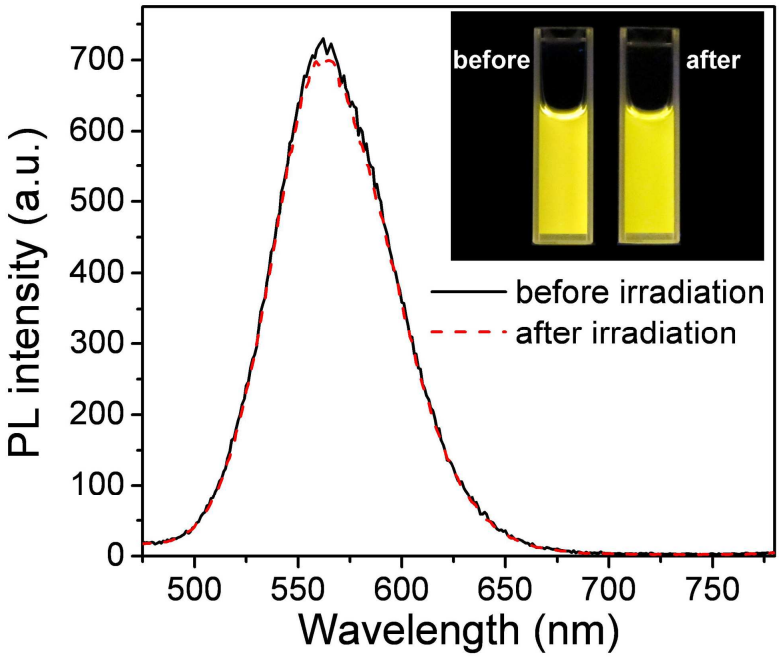

Figure S14. Time-resolved luminescence spectra of the CdTe QDs decorated with MPA (a), α-CD (b) and β-CD (c). The measurements are performed at room temperature with the excitation wavelength at 400 nm. (d) Summaries of the τ_1 and τ_2 in the equation $Y=Y_0+B_1\cdot\exp(-t/\tau_1)+B_2\cdot\exp(-t/\tau_2)$, which is used to fit the time-resolved luminescence spectra. No obvious difference is found for MPA-, α-CD- and β-CD-decorated CdTe QDs.

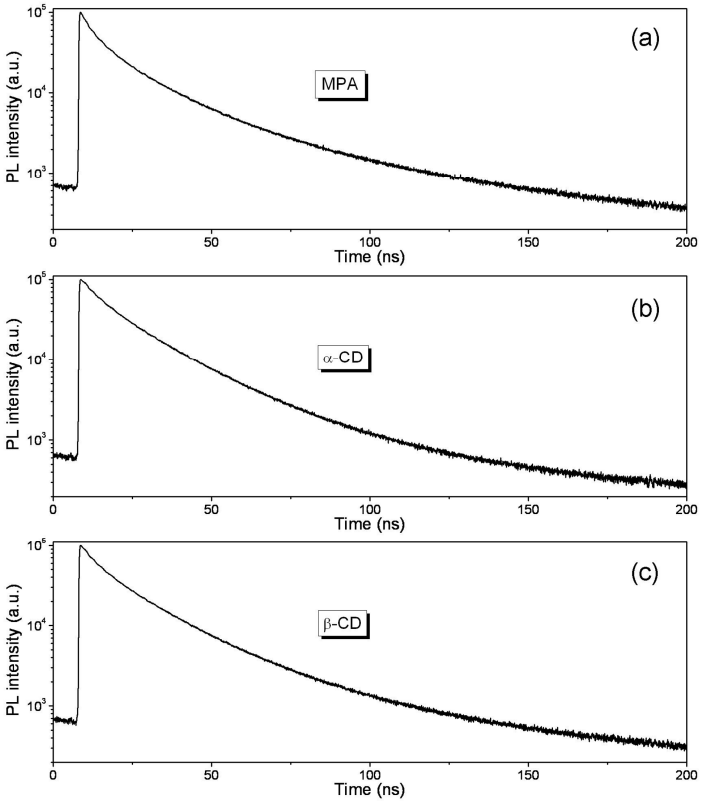

(d)

	MPA	α -CD	β -CD
τ_1 (ns)	5.582	6.154	5.988
τ_2 (ns)	25.12	21.87	22.93

References:

S1 Schneider, H.-J.; Hacket, F.; Rüdiger, V.; Ikeda, H. NMR Studies of Cyclodextrins and Cyclodextrin Complexes. *Chem. Rev.* **1998**, *98*, 1755-1786.

S2 Streefkerk, D.; De Bie, M.; Vliegenthart, J. Conformational Studies on Pertrimethylsilyl Derivatives of Some Mono- and Disaccharides by 220 MHz PMR Spectroscopy. *Tetrahedron* **1973**, *29*, 833-844.

S3 Wood, D. J.; Hruska, F. E.; Saenger, W. ^{1}H NMR Study of the Inclusion of Aromatic Molecules in α-Cyclodextrin. *J. Am. Chem. Soc.* **1977**, *99*, 1735-1740.

S4 Kozár, T.; Venanzi, C. A. Reconsidering the Conformational Flexibility of β-Cyclodextrin. *J. Mol. Struct.* **1997**, *395-396*, 451-468.

S5 Lipkowitz, K. B. Applications of Computational Chemistry to the Study of Cyclodextrins. *Chem. Rev.* **1998**, *98*, 1829-1873.

S6 Varshni, Y. P. Temperature Dependence of the Energy Gap in Semiconductors. *Physica* **1967**, *34*, 149-154.

S7 Joshi, A.; Narsingi, K. Y.; Manasreh, M. O.; Davis, E. A.; Weaver, B. D. Temperature Dependence of the Band Gap of Colloidal CdSe/ZnS Core/Shell Nanocrystals Embedded into an Ultraviolet Curable Resin. *Appl. Phys. Lett.* **2006**, *89*, 131907.

S8 Valerini, D.; Cretí, A.; Lomascolo, M.; Manna, L.; Cingolani, R.; Anni, M. Temperature Dependence of the Photoluminescence Properties of Colloidal CdSe/ZnS Core/Shell Quantum Dots Embedded in a Polystyrene Matrix. *Phys. Rev. B* **2005**, *71*, 235409.

S9 Yeon Woo, J.; Kumar Tripathy, S.; Kim, K.; Han, C. S. Thermal and Structural Dependence of the Band Gap of Quantum Dots Measured by a Transparent Film Heater. *Appl. Phys. Lett.* **2012**, *100*, 063105.

S10 Chin, P. T. K.; de Mello Donegá, C.; van Bavel, S. S.; Meskers, S. C. J.; Sommerdijk, N. A. J. M.; Janssen, R. A. J. Highly Luminescent CdTe/CdSe Colloidal Heteronanocrystals with Temperature-Dependent Emission Color. *J. Am. Chem. Soc.* **2007**, *129*, 14880-14886.

S11 Adachi, S. *Handbook on Physical Properties of Semiconductors*; Springer, 2004; Vol. 3.

S12 Liu, K.; Nie, Z. H.; Zhao, N. N.; Li, W.; Rubinstein, M.; Kumacheva, E. Step-Growth Polymerization of Inorganic Nanoparticles. *Science* **2010**, *329*, 197-200.